MOLECULAR AGGREGATES FOR ENHANCED PHOTOTHERMAL EFFECT

M.Sc. Thesis

By

RACHAYITA DAS

2303171005

DEPARTMENT OF BIOSCIENCES AND BIOMEDICAL ENGINEERING

INDIAN INSTITUTE OF TECHNOLOGY INDORE

MAY 2025

MOLECULAR AGGREGATES FOR ENHANCED PHOTOTHERMAL EFFECT

A THESIS

Submitted in partial fulfilment of the requirements for the award of the degree
of
Master of Science

by
RACHAYITA DAS

DEPARTMENT OF BIOSCIENCES AND BIOMEDICAL ENGINEERING
INDIAN INSTITUTE OF TECHNOLOGY INDORE
MAY 2025

INDIAN INSTITUTE OF TECHNOLOGY INDORE

CANDIDATE'S DECLARATION

I hereby certify that the work which is being presented in the thesis entitled **MOLECULAR AGGREGATES FOR ENHANCED PHOTOTHERMAL EFFECT** in the partial fulfillment of the requirements for the award of the degree of **MASTER OF SCIENCE** and submitted in the **DEPARTMENT OF BIOSCIENCES AND BIOMEDICAL ENGINEERING , Indian Institute of Technology Indore**, is an authentic record of my own work carried out during the time period from July 2024 to May 2025 under the supervision of Prof. Sharad Gupta, Professor.

The matter presented in this thesis has not been submitted by me for the award of any other degree of this or any other institute.

Rachayita Das 23.5.25
Signature of the student with date
(RACHAYITA DAS)

This is to certify that the above statement made by the candidate is correct to the best of my/our knowledge.

Sharad Gupta 23/05/2025
Signature of the Supervisor of
M.Sc. thesis (with date)

Prof. SHARAD GUPTA

RACHAYITA DAS has successfully given her M.Sc. Oral Examination held on **5 MAY 2025.**

Sharad Gupta 23/05/2025
Signature of Supervisor of MSc thesis
Date:

Convener, DPGC
Date: 23-05-2025

ACKNOWLEDGEMENTS

First and foremost, I would like to express my deepest gratitude to **Professor Sharad Gupta**, my supervisor, for his invaluable guidance, constant support, and encouragement throughout the course of this project. His expertise, insightful feedback, and thoughtful suggestions have been essential at every stage , from shaping the research questions to interpreting the results and I am truly grateful for the opportunity to learn under his mentorship.

I would also like to extend my heartfelt thanks to the **Dr. Parimal Kar**, **Head of the Department, Department of Biosciences and Biomedical Engineering (BSBE)**, and **Professor Prashant Kodgire**, **DPGC and BSBE Convener**, for providing the necessary infrastructure and support that made this work possible. I am grateful to all the **faculty members of the BSBE department** at IIT Indore for their teaching, constructive feedback, and inspiration during my academic journey.

Special thanks go to **Ms. Anusha Srivastava**, Ph.D. scholar in the lab, whose patient guidance, hands-on training, and helpful discussions were invaluable to my work. I am equally thankful to my senior lab mates - **Priyanka Payal** and **Neeraj Sati** and my batchmates **Surjyapratap Sarangi** and **Advait Sohani**, for their collaborative spirit, practical assistance, and constant support in both the lab and academic life.

I would also like to acknowledge the help provided by the **Sophisticated Instrumentation Center (SIC), IIT Indore**, whose facilities and staff played an essential role in characterizing the materials and performing critical analyses in this project.

Beyond the academic sphere, I am deeply grateful to **my father Chandan Das, my mother Susmita Das** and my friend **Somsubhra Goswami** for their endless love, encouragement, and belief in me. Their moral support has been the foundation of my resilience during

challenging moments and has kept me motivated throughout this research journey.

I am also thankful to Srija Mukherjee and Rima Sen, my friends at IIT Indore who have supported me a lot during this journey.

Last but not least, I thank **God** for granting me the strength, perseverance, and clarity needed to carry out this work.

DEDICATION

I would like to dedicate my M.Sc. thesis to my parents.

Abstract

Photothermal therapy (PTT) is emerging as a promising non-invasive cancer treatment which utilizes localized heat generation by near-infrared (NIR) light to cause tumor ablation. Indocyanine green (ICG) is an FDA approved NIR dye which has been widely used as a photothermal agent (PTA). The therapeutic potential of ICG is hindered by rapid degradation, rapid clearance from circulation and poor photostability. To address these limitations, recent studies are going on in J-aggregates which are the molecular assemblies of ICG arranged in a head to tail manner with a red shifted absorption spectrum. Our study explores the photophysical characteristics of J-aggregates. It also focuses on the formation and application of J-aggregates, which exhibit enhanced optical stability, improved heat generation, and superior photothermal conversion efficiency. A new approach has been followed to enhance the photothermal conversion efficiency by utilizing a dual-laser irradiation set up orchestrated using some optical tools. This report highlights the optimal concentration, temperature, incubation time for the formation of J-aggregates and its stability across different solvents and pH systems. In addition, the photothermal studies revealed a substantial increase in temperature elevation for J-aggregates under dual laser irradiation. Preliminary in-vitro cytotoxicity studies have shown high biocompatibility of J-aggregates in normal and cancer cells. However, In-vitro PTT study and life-dead assays also shown that J-aggregates are efficient photothermal agent for the killing of cancerous cells under dual laser irradiation. Thus, these findings bring that J-aggregates can be a promising photothermal agent for effective cancer treatment.

TABLE OF CONTENTS

LIST OF FIGURES

ACRONYMS

PTT: Photothermal therapy

ICG: Indocyanine green

PTA: Photothermal agent

NIR: Near infrared region

IVR PTT: In-vitro Photothermal therapy

PBS: Phosphate buffer solution

DAPI: 4',6-di-amidino-2-phenylindole

PI: Propidium iodide

MTT: 3-[4,5-dimethylthiazol-2-yl]-2,5 diphenyl tetrazolium bromide

TNBC: Triple negative breast cancer

Chapter 1

Introduction

1.1 Background of photothermal therapy (PTT)

Cancer remains one of the leading causes of mortality worldwide, with an estimated 20 million new cases and over 10 million cancer-related deaths reported in 2022, according to the WHO and Global Cancer Observatory (GLOBOCAN) [1]. Among all cancer types, breast cancer is the most commonly diagnosed globally, accounting for over 2.3 million new cases annually and standing as a major cause of cancer-related deaths among women [1]. Triple negative breast cancer, a particularly aggressive subtype, lacks estrogen, progesterone, and HER2 receptors, making it unresponsive to hormonal and targeted therapies [2]. Current treatment options for breast cancer—including surgery, chemotherapy, radiation, and hormone therapy—are associated with significant limitations, such as non-specific toxicity, systemic side effects, drug resistance, and poor long-term outcomes, particularly in TNBC cases [3]. These treatments often compromise quality of life and are insufficient in preventing recurrence or metastasis. As a result, there is a critical need for more effective and targeted therapeutic strategies. In this context, photothermal therapy has emerged as a promising alternative due to its minimally invasive nature and ability to kill cancer cells using near-infrared light and photothermal agents, thereby reducing off-target effects and enhancing therapeutic precision. Photothermal therapy is an emerging and promising approach for cancer treatment that utilizes the conversion of absorbed light energy into localized heat to induce the destruction of cancerous tissues [4]. Unlike traditional treatments such as chemotherapy or radiotherapy, which often affect both healthy and diseased tissues, photothermal therapy offers a minimally invasive, highly targeted, and minimally damaging alternative. The basic principle of PTT involves administering a photothermal agent into the tumor region, followed by the irradiation of the area with a laser in the near-infrared range [5]. The PTA absorbs the

laser light and converts it into heat, leading to localized hyperthermia that can selectively kill tumor cells while sparing surrounding healthy tissues. There are two steps in photothermal killing. One is hyperthermia and other is thermal ablation. Hyperthermia means increase in the temperature and thermal ablation is removal of the tumor by inducing thermal stress. The temperature rises up to 42^0C in hyperthermia which is maintained for a specific time and in other case of thermal ablation temperature increases more than 42^0C for few minutes [6]. It uses a photothermal agent which is capable to absorb light (particularly at near infrared region) and convert light energy to heat energy through non-radiative processes. This localized heat can be exploited to kill cancer cells in PTT.

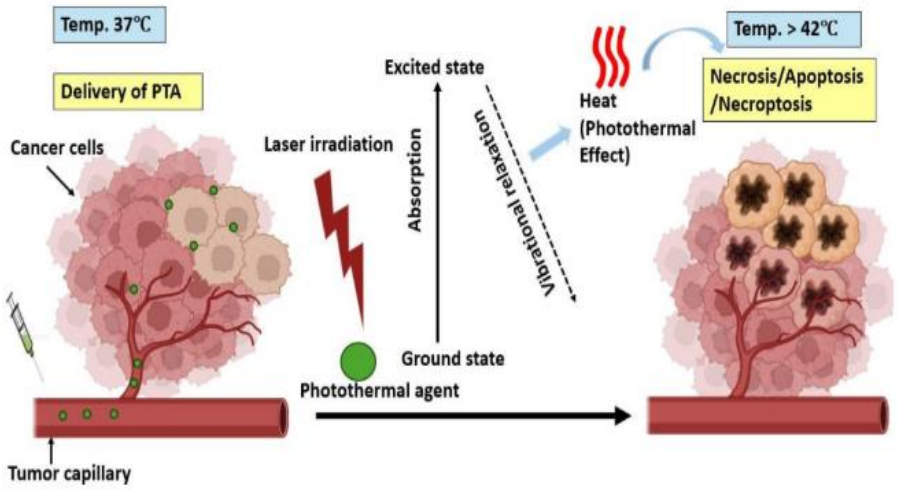

Figure 1. Mechanisms of photothermal therapy (*Created with Biorender*)

1.2 Mechanism of cellular death in photothermal therapy

Photothermal therapy induces cancer cell death primarily through two mechanisms: necrosis and apoptosis, depending on factors like the type of PTA, laser power, and irradiation time [7]. Necrosis results from high-energy irradiation, causing immediate loss of membrane integrity and the release of intracellular contents, which triggers inflammatory and immunogenic responses, generally undesirable in cancer treatment. In contrast, under controlled, lower-energy irradiation, PTT can induce

apoptosis, a regulated, non-inflammatory form of cell death driven mainly by the intrinsic (mitochondrial) pathway [7]. Here, heat stress activates pro-apoptotic proteins Bax and Bak, leading to mitochondrial membrane permeabilization, cytochrome c release, apoptosome formation, and activation of caspase-9 and caspase-3, which can ultimately result in orderly cell death and phagocytic clearance. Additionally, PTT can trigger lysosomal rupture, releasing cathepsins that cleave Bid, a pro-apoptotic protein, into its active form, further amplifying the apoptotic cascade[8].

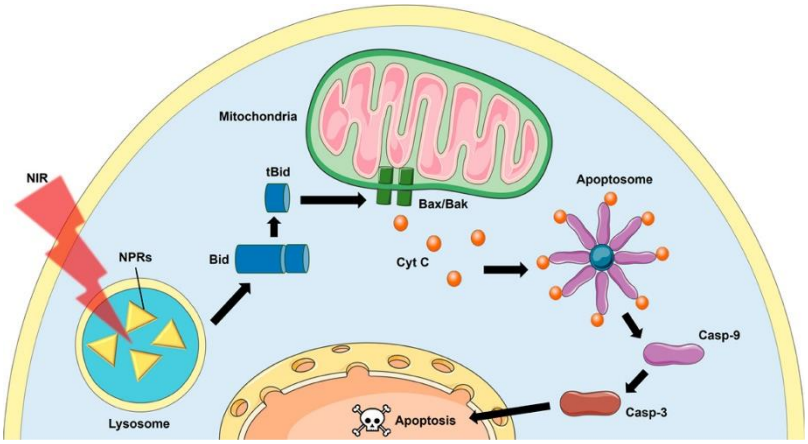

Figure 2. Mechanism of cell death in [8]

1.2 Near infrared based photothermal therapy

Near-infrared photothermal therapy is superior to visible light-based because NIR light penetrates deeper into biological tissues due to lower scattering and absorption [9]. This allows for more effective and targeted heating of tumors located beneath the skin surface, enhancing therapeutic outcomes while minimizing damage to surrounding healthy tissue. NIR light is classified into two windows: NIR-I (700–900 nm) and NIR-II (1000–1700 nm) [10]. The NIR-I window is characterized by reduced light scattering and minimal absorption by intrinsic biological chromophores like water, haemoglobin, and melanin, allowing for efficient penetration into tissues up to several centimetres deep [11]. The NIR-II window offers even greater advantages, such as lower scattering and deeper tissue penetration, providing superior spatial resolution and therapeutic efficacy for tumors located at significant

depths. Upon NIR laser irradiation, photothermal agents such as gold nanoparticles, carbon-based nanomaterials, and organic dyes absorb the light energy and convert it into heat, leading to localized hyperthermia that induces cancer cell apoptosis or necrosis without significantly harming surrounding healthy tissues. NIR-based PTT is highly attractive due to its high spatial precision, reduced systemic toxicity compared to chemotherapy, and the potential for real-time imaging-guided treatment [12]. Current research focuses on developing highly efficient, biocompatible photothermal agents and optimizing laser parameters to maximize therapeutic outcomes while minimizing side effects.

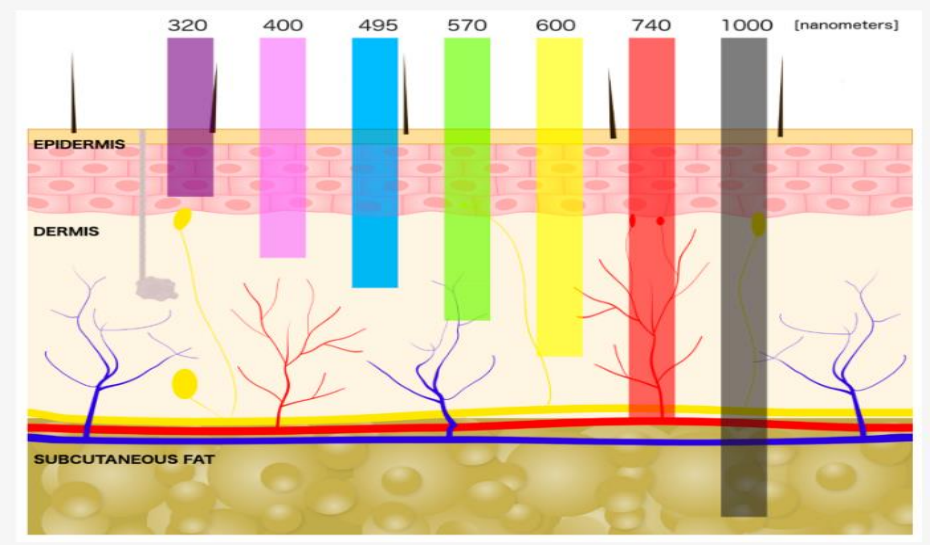

Figure 3. The skin layer showing dermal penetration by different wavelengths of light. [9]

1.4 Indocyanine green: a versatile NIR dye

ICG is an FDA-approved near-infrared (NIR) fluorescence dye widely used in the field of biomedical research, disease diagnostics, and therapeutics. Since its approval in the 1950s, ICG has gained prominence due to its excellent optical properties, biocompatibility, and versatility across applications in imaging[13]. ICG is a tri-carbocyanine dye with peak absorption around 780 nm and fluorescence emission around 820–840 nm in aqueous solutions[14]. These wavelengths fall within the "NIR optical window," where biological tissues have minimal absorption and scattering, which allows deep tissue penetration and high

signal-to-background ratios. This makes ICG especially valuable for in vivo imaging, such as fluorescence-guided surgery, lymph node mapping, angiography, and tumor visualization. Besides it's imaging property, ICG is also used as a photothermal agent due to its strong absorption efficiency. When irradiated with NIR laser light, ICG molecules absorb photons and undergo nonradiative decay, releasing the absorbed energy as heat. This photothermal conversion leads to a local temperature rise that can induce cellular damage, protein denaturation, and ultimately apoptosis or necrosis of cancer cells. One advantage of using ICG over other inorganic photothermal agents (like gold nanorods or carbon nanotubes) is its biodegradability and renal or hepatic clearance, reducing concerns about long-term toxicity[15]. However, free ICG in solution has some limitations. It is prone to photobleaching, rapid degradation in aqueous environments, and short blood circulation

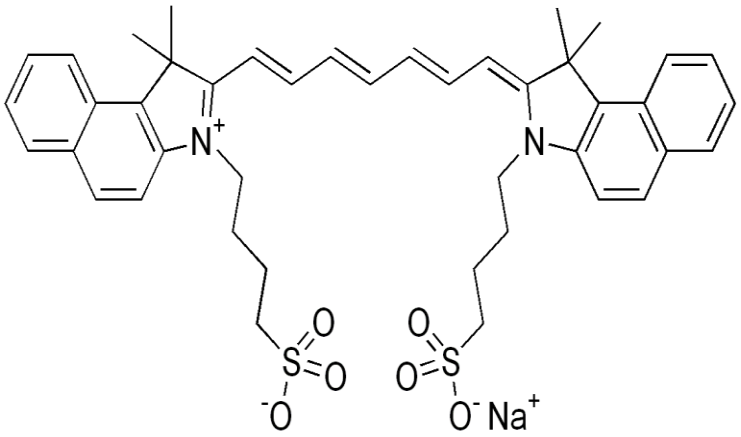

Figure 4. Molecular structure of ICG

time (half-life ~3–5 minutes).

1.5 Aggregation of ICG

Under external effect (like effect of solvent, salt, pH, temperature etc.) ICG can form two distinct type of molecular aggregation (H and J aggregates) which has unique optical properties [16]. **J-aggregates** are characterized by a red-shifted absorption peak relative to the monomer, enhanced photothermal conversion efficiency, and improved photostability, making them ideal for photothermal therapy and other biomedical applications [17]. These aggregates arise due to head-to-tail

molecular arrangements that promote constructive excitonic coupling, leading to bathochromic shift. In contrast, **H-aggregates** result from a face-to-face stacking arrangement, leading to a blue-shifted absorption peak by hypsochromic shift [18]. The formation of J- or H-aggregates is influenced by factors such as concentration, solvent polarity, pH, temperature, and the presence of surfactants or nanocarriers. While J-aggregates enhance the therapeutic utility of ICG, H-aggregates are often undesirable in PTT due to their lower efficiency. J-aggregates exhibit superior photothermal conversion efficiency compared to H-aggregates due to their distinct molecular arrangement [19]. In J-aggregates, dye molecules align in a head-to-tail fashion, which leads to a red-shifted and narrowed absorption band with enhanced oscillator strength. This configuration promotes stronger and more efficient light absorption in the NIR region and facilitates exciton delocalization, enhancing non-radiative decay pathways essential for photothermal conversion. In contrast, H-aggregates adopt a face-to-face stacking, resulting in blue-shifted absorption and exciton coupling that favours radiative decay, thus limiting their photothermal efficiency [20].

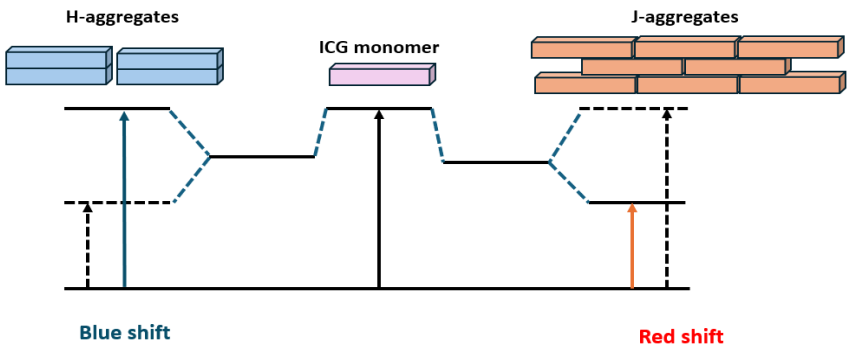

Figure 5. Aggregation of ICG

1.6 Indocyanine Green J-aggregates

ICG J-aggregates are specialized molecular assemblies formed by the head-to-tail arrangement of indocyanine green (ICG) molecules, resulting in unique optical and therapeutic properties. Unlike monomeric ICG, J-aggregates exhibit a red-shifted absorption peak

(around 896 nm), which enhances their ability to absorb light in the near-infrared (NIR) region, particularly beneficial for applications like photothermal therapy (PTT). These aggregates can have improved photothermal conversion efficiency, higher photostability, making them superior for heat generation in cancer ablation therapies [21]. The formation of J-aggregates is influenced by environmental factors such as pH, ionic strength, temperature, and concentration, as well as interactions with stabilizing carriers like nanoparticles or surfactants [21]. By leveraging these properties, J-aggregates overcome some of the inherent limitations of monomeric ICG, such as rapid degradation and poor stability, making them a promising photothermal agent.

Chapter 2

Literature review

2.1 Background study

Photothermal therapy (PTT) has emerged as a promising minimally invasive approach for cancer treatment, leveraging the ability of specialized materials to convert light energy—typically in the near-infrared (NIR) range—into localized heat that can ablate tumor tissues. Among various photothermal agents explored, molecular chromophores like indocyanine green (ICG) and other cyanine derivatives have attracted considerable attention due to their strong NIR absorption, biocompatibility, and clinical approval. A particularly exciting development in this area is the use of J-aggregates—highly ordered molecular assemblies formed through the self-organization of dye molecules—as efficient photothermal transducers.

J-aggregates are formed when dye molecules, under appropriate conditions (e.g., high concentration, salt presence, controlled temperature, pH adjustment), align in a head-to-tail fashion driven by π–π stacking and hydrophobic interactions[22]. This organization leads to distinct optical properties compared to dye monomers, most notably a sharp, red-shifted absorption peak and significantly enhanced photostability. For ICG, monomers absorb around 780 nm, while J-aggregates display a shifted peak near 896 nm, placing them deeper into the NIR window, where biological tissue transparency is highest. This shift not only improves light penetration but also enhances photothermal conversion efficiency, making J-aggregates particularly attractive for in vivo applications.

Early studies investigating cyanine dye aggregates focused on their unique spectroscopic behaviour, but more recent research has pivoted toward their biomedical applications. The enhanced thermal stability and reduced photobleaching of these aggregates address a key limitation of free ICG, which degrades rapidly under continuous irradiation.

Moreover, the nanoscale size of ICG J-aggrgates (typically 50–200 nm) promotes passive accumulation in tumors through the enhanced permeability and retention (EPR) effect, further improving PTT selectivity[23].

2.2 Methods of J-Aggregate Formation

Indocyanine Green (ICG) J-aggregates can be formed through various methods like temperature and concentration induced aggregation, metal ion induced aggregation, micelle assisted aggregation, and liposome encapsulation. Each of these methods have unique advantages and limitations. Among these methods temperature induced J-aggregates formation is highly simple and cost-effective. In this method J-aggregates are formed in a controlled environment for example heating ICG solutions at 60°C for 24 hours results in stable J-aggregates with a characteristic absorption peak around 896 nm [24]. These J-aggregates are more biocompatible, as they do not contain potentially toxic metal ions, surfactants, or lipid carriers that could trigger immune responses or toxicity. Additionally, these J-aggregates can be stabilized without external carriers by adjusting temperature and ionic strength which can ensure long-term stability in biological environments. Some metal ions like Mg^{2+} and Fe^{2+}, can induce J-aggregation by promoting dye-dye stacking. While this method stabilizes aggregates but it has potential biocompatibility concerns, as excess metal ions can lead to toxicity [25]. In micelle-assisted J-aggregates, surfactants such as Pluronic F127 or SDS create micelles that encapsulate ICG, inducing controlled aggregation [26]. Micelle-based aggregates may improve dye stability and solubility but may suffer from dilution-induced disassembly in biological environments. In liposome induced J-aggregation, ICG is embedded into lipid bilayer but it is costly and the process of formation is very complex.

2.2.1 Aqueous Solution-Induced J-Aggregation

This is the most straightforward and widely used approach, relying on manipulating basic solution conditions. Generally, heating aqueous ICG

solutions under controlled pH, ionic strength, and concentration can promote spontaneous self-assembly into J-aggregates. These aggregates exhibit a red-shifted absorption peak (~895–920 nm) compared to monomeric ICG (~780 nm), enhancing tissue imaging and phototherapy capabilities [16]. The major advantages of this method include its simplicity, low cost, and high biocompatibility, as no foreign materials are required.

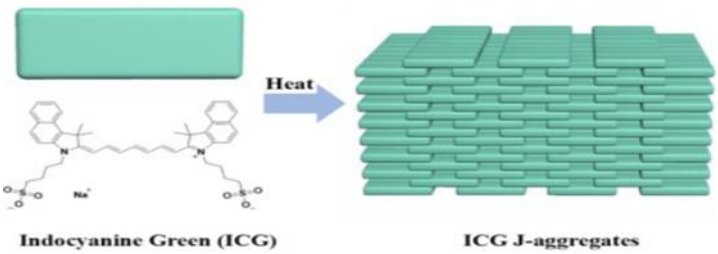

Figure 6. Aqueous solvent induced J-aggregation [16]

2.2.2 Metal-Ion Induced J-Aggregation

Metal-ion-induced aggregation uses divalent or trivalent metal ions (e.g., Mg^{2+}, Ca^{2+}, Ba^{2+}) to promote stacking through ionic interactions. Introduction of Mg^{2+} or Ca^{2+} into ICG solutions reduces electrostatic repulsion and promotes closer packing, enhancing J-aggregate formation[25]. This method provides tunability over aggregate size and optical properties by adjusting ion type and concentration. However, it comes with notable challenges, including potential in vivo toxicity from

excess metal ions, interference from endogenous biological ions, and limited aggregate stability under physiological conditions [25].

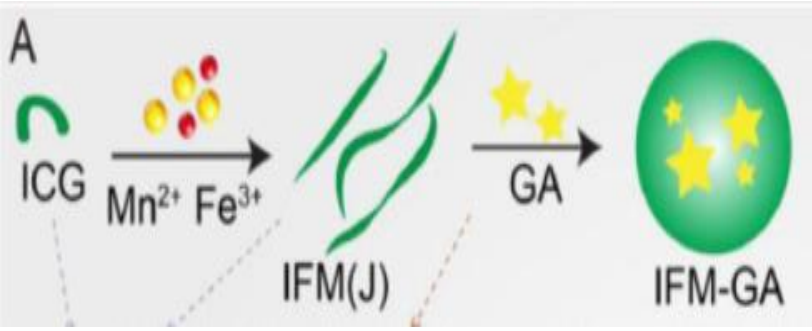

Figure 7. Metal ion induced J-aggregation [25]

2.2.3 Micelle-Assisted J-Aggregation

Micellar systems, using surfactants like sodium dodecyl sulfate (SDS) or block copolymers such as Pluronic F127, can encapsulate ICG and promote aggregation. It is reported that micelle-encapsulated ICG J-aggregates show improved solubility, photostability, and spectral performance compared to free dye [27]. Additionally, micelle-based systems can be surface-functionalized for targeted delivery. However, they are inherently sensitive to dilution, as micelle integrity depends on maintaining concentrations above the critical micelle concentration (CMC), and surfactant residues may raise cytotoxicity concerns depending on the formulation [27].

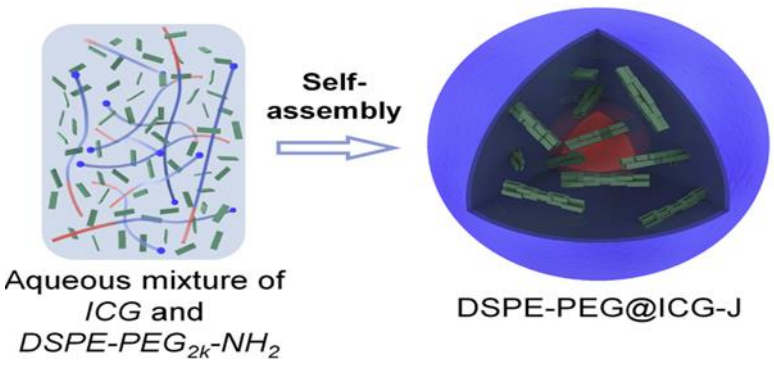

Figure 8. Michelle induced J-aggregation [27]

2.2.4 Chemical induced J-aggregation

A more recent and innovative approach involves using hydrophobic or amphiphilic drug molecules to induce or co-assemble with ICG into J-aggregates. It was demonstrated that co-loading ICG with chemotherapeutic agents such as paclitaxel or doxorubicin in a shared nanocarrier or solution can promote cooperative aggregation [28]. This happens because hydrophobic drug molecules facilitate dye stacking through hydrophobic interactions and π–π stacking, enhancing optical properties while enabling simultaneous drug delivery and imaging (theragnostic). Drug-induced aggregation systems provide a multifunctional platform combining imaging, therapy, and controlled release. However, the aggregation behaviour can be highly dependent on drug-to-dye ratios, solvent environment, and carrier material, making system optimization complex [17]. Additionally, potential interactions between the drug and dye need to be carefully evaluated to ensure preserved therapeutic activity and stability.

In this work, we focus specifically on temperature-induced J-aggregation of ICG as the method of choice for generating stable J-aggregates. Among the various reported strategies including metal-ion induction, micelle-assisted assembly, and drug-induced aggregation the temperature-based aqueous approach offers a particularly attractive balance of simplicity, cost-effectiveness, and biocompatibility. By carefully heating aqueous ICG solutions under controlled conditions, we can promote the spontaneous self-assembly of ICG molecules into highly ordered J-aggregates characterized by a distinct red-shifted absorption peak (896 nm), enhanced photothermal conversion efficiency, and improved photostability compared to the monomeric dye. One of the major advantages of this method is that it avoids the need for external surfactants, polymers, or metal ions, thereby minimizing biocompatibility concerns and simplifying downstream purification. Additionally, the scalability of this method makes it particularly suitable for laboratory optimization and eventual translation into *in-vivo* applications. In our lab, we have optimized the key

parameters influencing aggregate formation — including dye concentration, heating duration, and temperature— to achieve reproducible, stable J-aggregates with tailored optical properties for biomedical use. This temperature-induced method not only provides a robust platform for fabricating stable J-aggregates but also lays the groundwork for the development of photothermal therapy agents with enhanced performance mediated by J-aggregates.

Chapter-3

Objectives

This study aimed to explore the potential of ICG J-aggregates as enhanced agents for photothermal cancer therapy by addressing three key objectives.

- **Objective 1:** The first objective was to synthesize, characterize, and assess the stability of ICG J-aggregates. This included optimizing the preparation conditions, such as temperature and incubation time, and systematically evaluating their stability under various environmental conditions (including storage time, pH, and solvent effects) to ensure reproducible and robust aggregate formation.

- **Objective 2:** The second objective focused on evaluating the ex-vitro photothermal performance of the synthesized J-aggregates. Using dual-laser irradiation (808 nm and 915 nm), we compared the temperature elevation and photothermal conversion efficiency of J-aggregates against free ICG to determine the superior light-to-heat conversion potential of the aggregated form.

- **Objective 3:** The third objective was to validate the photothermal therapeutic effect of ICG J-aggregates *in-vitro*. We examined cellular uptake, assessed inherent cytotoxicity without laser exposure, and measured cancer cell-killing efficiency using *in-vitro* photothermal cytotoxicity assessment and fluorescence based live-dead assay following laser irradiation. Together, these objectives aimed to establish ICG J-aggregates as promising candidates for precise, efficient, and minimally invasive photothermal cancer treatments.

Chapter 4

Materials and methods

4.1 Materials

Indocyanine green (ICG) was purchased from Sigma-Aldrich. Absolute ethanol, acetone and chloroform were purchased from Merck Life science private Ltd. PBS buffer reagents containing sodium chloride (NaCl), potassium chloride (KCl), disodium hydrogen phosphate (Na_2HPO_4) and potassium dihydrogen phosphate (KH_2PO_4) were purchased from Thomas Baker (Mumbai). Dimethyl sulfoxide (DMSO) was purchased from MP Biomedicals LLC. Dulbecco's Modified Eagle Medium (DMEM), fetal bovine serum (FBS), penicillin-streptomycin, 0.25% trypsin–1 mM ethylenediaminetetraacetic acid (EDTA), and 2.5% trypsin were purchased from Gibco. MTT (3-(4,5-dimethylthiazol-2-yl)-2,5-diphenyltetrazolium bromide) and DAPI dihydrochloride were procured from Himedia. Calcein-AM was purchased from Merck and Propidium Iodide was purchased Thermo Fisher Scientific.

4.2 Methods

4.2.1 Preparation of ICG J-aggregates

To check the optimum concentration for the formation of J-aggregates ICG solutions of different concentrations ranging from 200 μM to 1 mM were prepared in autoclaved milli-Q water. The samples were taken in different microcentrifuge tubes and incubated at 60°C in a heating block for 24 hours. The absorption spectra of each sample was recorded to check the optimum concentration for J-aggregates formation. The effect of temperature in the formation of J-aggregates was checked. The optimized ICG concentrations were taken in different MCTs and incubated at different temperatures ranging from 40°C to 80°C. UV-Visible spectrophotometer was used to record the absorption spectra following incubation in order to detect the red-shifted absorption peak, which is usually located between 890 and 900 nm and is suggestive of

J- aggregation. To study the effect of incubation time on the formation of ICG J-aggregates, ICG solutions at optimal temperature (from previous experiment) were incubated at varying time intervals (e.g., 6, 12, 24, 36, 48 hours). After each incubation period, aliquots were taken and the absorption spectra were measured using a UV-Vis spectrophotometer to monitor the development of the red-shifted absorption peak, characteristic of J-aggregates (~890–900 nm).

4.2.2 Stability assessment of ICG J-aggregates

J-aggregates were prepared in optimized temperature for the optimized incubation time. After the formation of J-aggregates, the solution was stored at 4°C for various time intervals (e.g., 12, 24, 36, 48 hours). At each time point, aliquots were taken and the absorption spectra was measured using a UV-Vis spectrophotometer to assess the stability of the J-aggregates by monitoring the persistence of the red-shifted absorption peak (~890–900 nm) and any changes in intensity. The percentage of J-aggregates present in each time point was calculated.

4.2.3 Photostability assessment of ICG J-aggregates

The photostability of ICG J-aggregates were compared with free ICG under continuous light exposure. Both free ICG and ICG J-aggregates were exposed to continuous light under normal room lighting conditions for different time intervals (e.g., 12, 24, 36, and 48 hours) while maintaining constant temperature. At each time point, aliquots are taken, and the absorption spectra were recorded using UV-Vis spectrophotometry, focusing on the characteristic absorption peaks of free ICG (~780 nm) and J-aggregates (~890–900 nm). The photostability was assessed by comparing the intensity changes in the absorption peaks, with time.

4.2.4 Effect of solvent on the stability of ICG J-aggregates

To check the effect of different solvents on ICG J-aggregates, solutions were prepared by dissolving 20 µL of ICG J-aggregates (12 µM) in 980 µL of various solvents of differing polarity and hydrogen bonding

capacity, including water, ethanol, acetone, chloroform, dimethyl sulfoxide (DMSO), and phosphate-buffered saline (PBS) in different MCTs. Absorption spectra were recorded using a UV-Vis spectrophotometer to check the stability of J-aggregates in different solvents.

4.2.5 Effect of pH on the stability of ICG J-aggregates

To check the effect pH on the stability of ICG J-aggregates, four pH solutions, which are generally present in tumor microenvironment i.e.8, 7.4, 6.8, 5.5, 4 were prepared. 20 µL ICG J-aggregates were taken in 980 µL of each pH solution. The J-aggregates were incubated in different pH solutions for 6 hours at 4°C. Absorption spectra were recorded using a UV-Vis spectrophotometer to check the stability of J-aggregates in different pH.

4.2.6 Study of photothermal effect of ICG J-aggregate

20 µM of ICG and J-aggregates of ICG solutions were prepared in deionized water. For each sample, aliquots of free ICG and ICG J-aggregates were placed in separate MCTs and exposed to 808 nm, 915 nm, and both lasers (808 nm + 915 nm) sequentially. The lasers were set to a specific power output of 1W, and the samples are irradiated for 5 minutes laser on and off condition. The temperature increase of each sample is monitored in real-time using a thermocouple. The temperature rise is recorded every 1 minute during laser irradiation. After irradiation, the maximum temperature achieved by each sample was analyzed and plotted.

4.2.7 Dual laser photothermal effect study

To investigate the photothermal effect under dual laser sources simultaneously, a continuous-wave 808 nm NIR laser and a continuous-wave 915 nm NIR laser, each with adjustable power densities were set up in a such way that the two beam spots co-axially overlapped. A long pass dichroic mirror was used, which passes the longer wavelength and reflects shorter wavelength. The laser beams were to irradiate the sample

area uniformly, ensuring overlap of the two wavelengths on the J-aggregate solution (Figure 9). Firstly, to optimize the power ratio (808 nm: 915 nm), different combination of power was taken in such a way so that the total power output remains 1 watt. Irradiation was applied for 15 minutes, and the temperature change (ΔT) was recorded every minute using a calibrated digital thermocouple probe inserted directly into the solution. Then for checking the effect of concentration in PTT, 6 different concentrations of J-aggregates were taken ranging from 20 to 70 µM. Measurement of temperature elevation was taken similarly. For thermal imaging, an infrared thermal camera (FLUKE) was also used to visualize heat distribution across the MCT. In the similar way the effect of laser power ranging from 0.5 watt to 2 watt were used to irradiate 20µM of J-aggregates and measurement of the temperature used similarly.

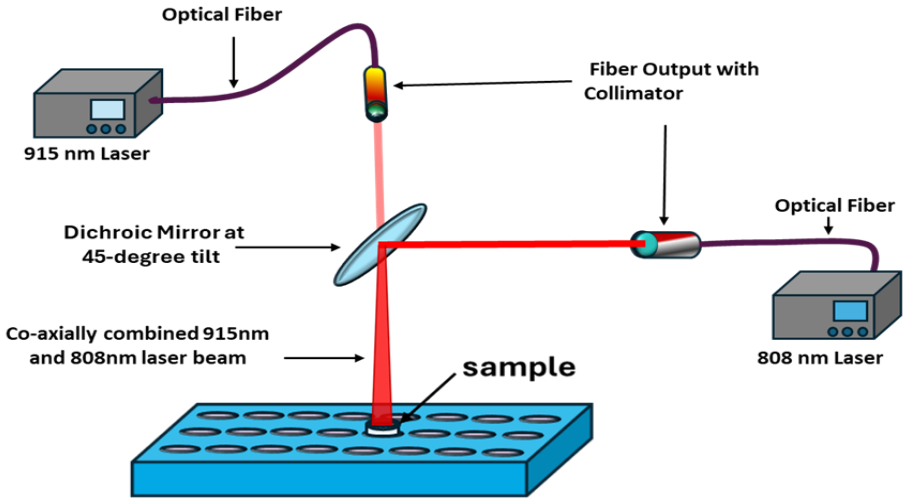

Figure 9. Dual laser set up

4.2.8. Cell culture

MDA-MB 231 cell line was used for all cell culture studies. DMEM with 1% Penicillin-streptomycin, 10% fetal bovine serum (FBS) was used to grow cells. Cells were cultured and incubated in a humidified environment with 5% carbon di oxide (CO2) at 37ºC. The cells were

detached with 0.25% trypsin-EDTA and sub cultured when they achieved around 80% confluency.

4.2.8.1 Cellular uptake and cytotoxicity study of J-aggregates

1×10^4 live cells per well were seeded in 96-well plate and allowed to grow for 24 hours. After 24 hours, samples were treated with ICG J-aggregates at various concentrations (20, 30, 40, 50, 60 and 70 μM) and incubated at 370C for 24 hours. The cells with only DMEM media and no J-aggregates was used as a positive control. The cell viability was assessed using standard MTT assay. Following 24 hours incubation period, 200 μL of MTT (0.5 mg/mL) was added in each well after aspirating off the J-aggregates. After 4 hours of incubation, 100 μL of DMSO was given to each well to dissolve the insoluble formazan crystals that the living cells had formed. The absorbance measurements were made at 570 nm using UV-Visible microplate spectrophotometer (SynergyH1, BioTek). The percentage drop in cell viability was measured.

NIR fluorescence imaging was carried out to evaluate the uptake of ICG J-aggregates by the MDA-MB 231 cells. Cells were cultured and seeded in 12 well plate (7000 cells per well) and were allowed to adhere for 24 hours. Following this, cells were incubated with 30 μM concentration of J-aggregates for 8 hours of incubation at 37^0C with 5% CO2 supply. Following incubation, the cells were washed thrice with PBS and cell fixation was done using 4% PFA for 20 minutes. Following this, PFA was removed and cells were washed again using PBS. The nucleus of the cells was stained with 1 μg/ml of DAPI. The cells were washed again with 1X PBS to remove extra dye. The NIR fluorescence imaging of MDA-MB 231 cells was done using Nikon Eclipse Ti-U inverted microscope equipped with xenon and mercury lamp along with UV and NIR filter cubes.

4.2.8.2 In-vitro PTT assessment

MDA-MB 231 cells were seeded in 96 well plates in which each well had 1×10^4 live cells. Cells were grown for 24 hours and then media was aspirated off. The cells were treated with different concentrations of J-aggregates ranging. Cells were incubated with J-aggregates and irradiated with dual laser at power 1 watt and 0.5 watt for 5 minutes. Cell viability was determined by MTT assay.

4.2.8.3 Live-dead assay

Calcein-AM and propidium iodide (PI) co-staining was done to assess the ratio of live and dead cells post incubation with ICG J-aggregates. Calcein is permeable to live cells where it is cleaved by the esterase cleave the acetoxymethyl groups from Calcein-AM and resulting in the formation of Calcein, which is a green fluorescent molecule. Calcein is retained in cells because of it's hydrophilic nature. Propidium iodide is a red fluorescent dye which is non permeable to live cells but can penetrate in dead or dying cell membrane. PI intercalates with nucleic acid and emits red fluorescence after binding. Live cells with intact membrane appear green under fluorescence microscopy and dead cells appears red.

In this experiment, 1.5×10^4 cells per well were seeded and grown for 24 hours. The cells were incubated with 20 μM of J-aggregates for 8 hours. After that cells were irradiated with dual laser for 5 minutes and after that co-stained with Calcein and PI. Cells without treatment was taken as control.

Chapter 5

Results and discussions

5.1 Synthesis of ICG J-aggregates

The first objective of this study was to optimize the conditions required to reproducibly synthesize stable J-aggregates of indocyanine green (ICG), a near-infrared (NIR) dye with applications in imaging and photothermal therapy. We systematically varied three parameters: concentration, temperature and incubation time and checked it's influence on spectral profile of J-aggregates using UV-Visible absorbance spectroscopy.

5.1.1 Concentration optimization

ICG solutions ranging from 200 μM to 1 mM were prepared to investigate the influence of concentration on J-aggregate formation. UV-Vis spectroscopy revealed a progressive increase in the characteristic red-shifted J-band (~896 nm) with rising concentrations, indicating enhanced aggregate formation. In figure 10(a) it is shown that the highest J-aggregate-to-monomer absorbance ratio was observed at 600 μM, suggesting this as the optimal concentration for stable and ordered self-assembly. These findings highlight that concentration is a critical parameter in tuning the photophysical behaviour of ICG, and optimizing it is essential for maximizing the formation and functional performance of J-aggregates in photothermal applications.

5.1.2 Temperature Optimization

ICG was incubated at different temperatures (40°C, 50°C, 60°C, 70°C and 80°C) to optimize ICG J-aggregate synthesis, monitoring the changes in absorbance intensity and spectral profile by UV-Vis spectroscopy. It is shown at figure 10(b) that at 40°C no aggregation was detected and in 50°C, minimal aggregation was detected, with only a faint shoulder near ~896 nm. At 60°C, we observed a strong, sharp absorbance peak at 896 nm, characteristic of J-aggregates, indicating

that the elevated temperature provided enough molecular motion to promote the π–π stacking and head-to-tail arrangement necessary for aggregate formation. However, at 70°C and higher temperature the peak intensity declined, likely due to thermal disruption of the non-covalent interactions holding the aggregates together, leading to partial disassembly or disordered aggregation. Thus, 60°C was identified as the optimal temperature for stable J-aggregate synthesis.

5.1.3 Optimization of Incubation Time

ICG solutions were incubated at 60°C for varying time period and absorbance was measured over time. Initial measurements at 6 hours showed weak aggregate signatures. At 12 hours, the 896 nm peak increased notably, reflecting significant aggregate formation. By 24 hours, the absorbance plateaued, and extending incubation to 36 hours produced no further gain, indicating that the system had reached equilibrium. The absorbance ration at 896 nm to 780 nm was found highest at 24 hours (Figure 10(c)). Therefore, a 24-hour incubation period was optimal for achieving complete and reproducible J-aggregates formation.

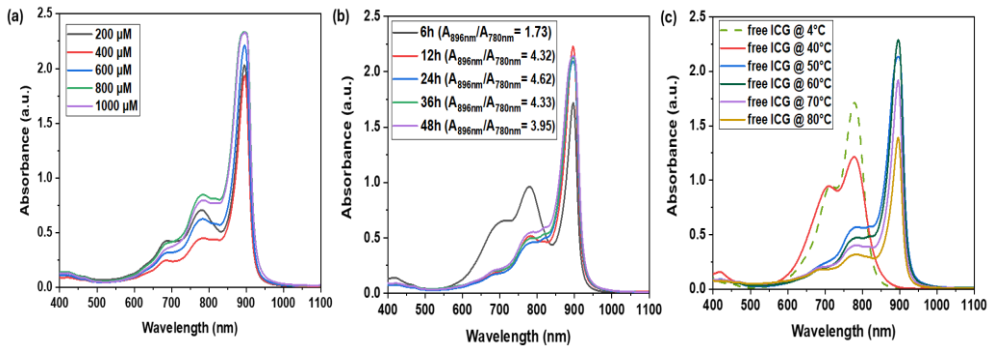

Figure 10. Absorbance spectra of (a) different concentrations of ICG kept at 60 °C for 24 h' to induce J aggregate formation (b) ICG J aggregates formed using 600 µM of ICG at different incubation times keeping incubation temperature constant at 60 °C, (c) ICG J aggregates formed using 600 µM of ICG at different incubation temperatures keeping incubation time constant at 24 h

5.2 Stability assessment of J-aggregates

5.2.1 Stability at 4ºC

The spectroscopic data (Figure 11(a)) showed that the aggregates remained stable for up to 48 hours when stored at 4°C, as indicated by minimal changes in the red-shifted absorption peak at 896 nm. It was calculated that even after 48 hours the intensity of ICG J-aggregates were still nearly 85% which indicates ICG J-aggregates are stable in 4^0C.

5.2.2 Photostability of ICG J-aggregates

The spectroscopic data (Figure 11(b)) revealed that J-aggregates exhibited significantly enhanced resistance to photodegradation under continuous light exposure. Free ICG showed a rapid decline in its characteristic absorption peak (~780 nm) within the first 6 hours of light exposure, indicating significant degradation. In contrast, ICG J-aggregates maintained their red-shifted absorption peak at 896 nm with only a minimal decrease in intensity over the same period, demonstrating superior stability. The enhanced photostability of J-aggregates can be attributed to their aggregated structure.

5.2.3 Stability of ICG J-aggregates in different solvent

Spectroscopic data revealed (Figure 11(c))when J-aggregates were exposed to organic solvents such as ethanol, acetone or DMSO, the characteristic 896 nm peak disappeared, and the spectrum reverted to the broad monomeric ICG peak (~780 nm). This suggests that organic solvents disrupt the hydrophobic interactions and π–π stacking that stabilize the aggregates. Specifically, reduced medium polarity and solvent-induced solvation effects weaken the non-covalent forces, leading to disassembly of the ordered J-aggregate structures into free ICG monomers. This sensitivity highlights a key limitation for formulation design: J-aggregates require aqueous conditions for stability.

5.2.4 pH stability of ICG J-aggregates

Spectroscopic data (Figure 11 (d)) showed that the J-aggregates were stable across acidic to mild basic conditions (pH 4–8), mimicking the tumor microenvironment. In case of monomeric ICG the at neutral or basic pH, after incubation in different pH solutions for stability of ICG decreases. Lowering pH induces J-aggregation in free ICG.

However, when the pH decreases (becomes acidic), the proton concentration increases, and some of the sulfonate groups ($–SO_3^-$) get protonated or at least have reduced negative charge density. This reduction in surface charge lowers the electrostatic repulsion, allowing the ICG molecules to approach each other more closely. Once they can pack together, π–π stacking interactions and hydrophobic forces dominate, driving the molecules into an ordered, slip-stacked J-aggregate structure [29].

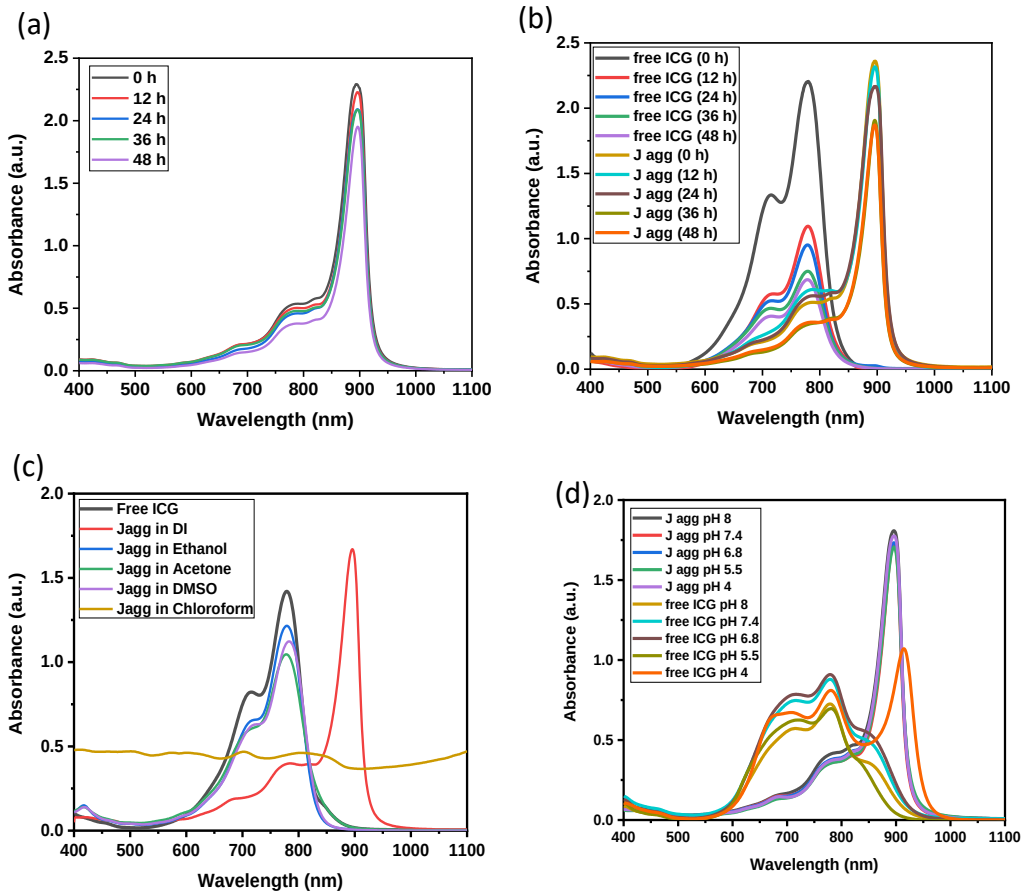

Figure 11. (a) Stability assessment of ICG J-aggregates stored at 4 °C for varying time periods (b) Optical stability assessment of free ICG and ICG J aggregates in MQ water kept at room temperature in well illuminated environment for varying time. (c) Absorbance spectral profile of ICG J aggregates in different organic solvents (d) comparative assessment of aqueous stability of free ICG and ICG J-aggregates after 6 h incubation with different pH solutions.

5.3 Study of photothermal effect of ICG J-aggregates

Figure 12 (a) shows the normalised spectra of free ICG and Figure 12 (b) shows normalised spectra of J-aggregates. Under continuous laser illumination, J-aggregates exhibited markedly higher temperature elevation compared to free ICG in 5 min laser on-off cycle (Figure 12(d)). J-aggregates retain their optical absorbance and structural integrity over time. Free ICG molecules photobleached rapidly, showing a decline in absorbance, likely due to their greater molecular freedom and higher susceptibility to reactive photoproduct formation (Figure 12 (c). This enhanced stability under light stress makes J-aggregates particularly suited for repeated or prolonged photothermal therapy.

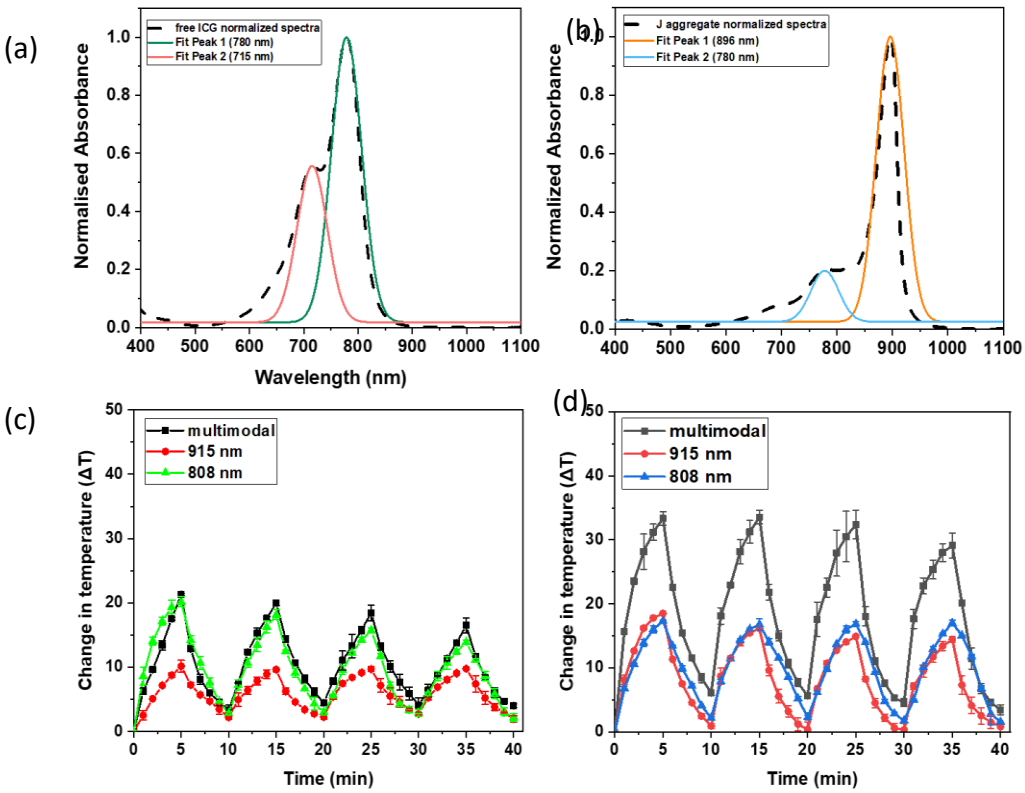

Figure 12. Normalized Absorption spectra of (a) free ICG and (b) ICG J aggregates. *ex vitro* photothermal temperature rise measured over four consecutive laser ON/OFF cycle for (c) free ICG (20 µM) and (d) ICG J aggregates (20 µM) under simultaneous dual-laser (multimodal), 915 nm laser, and 808 nm laser, respectively.

5.4 Dual laser photothermal effect study

We used dual laser irradiation specifically combining 808 nm and 915 nm wavelength to enhance the photothermal efficiency of ICG J-aggregates by taking advantage of their broad NIR absorption profile. Additionally, dual-wavelength irradiation may allow for deeper tissue penetration and more effective energy distribution, which is especially beneficial in therapeutic applications where uniform heating and maximized photothermal conversion are critical. This approach also helps overcome the limitations of single-laser systems, such as insufficient heating or rapid signal drop-off due to photobleaching or spectral mismatch.

Different concentration of ICG J-aggregates affects temperature elevation under dual-laser (808 + 915 nm) irradiation. As the J-aggregate concentration increased, the photothermal effect became more pronounced, with higher concentrations producing greater temperature rises (Figure 13 (a)). This reflects the larger total absorbance cross-section and greater photon capture at higher dye concentrations, enhancing overall light-to-heat conversion efficiency. Similarly, IR thermal images (Figure 13 (C)) also revealed concentration dependent heating. Similarly, increasing the laser power led to a proportional rise in the temperature (Figure 13 (b)), demonstrating that photothermal conversion efficiency is strongly dependent on the energy input.

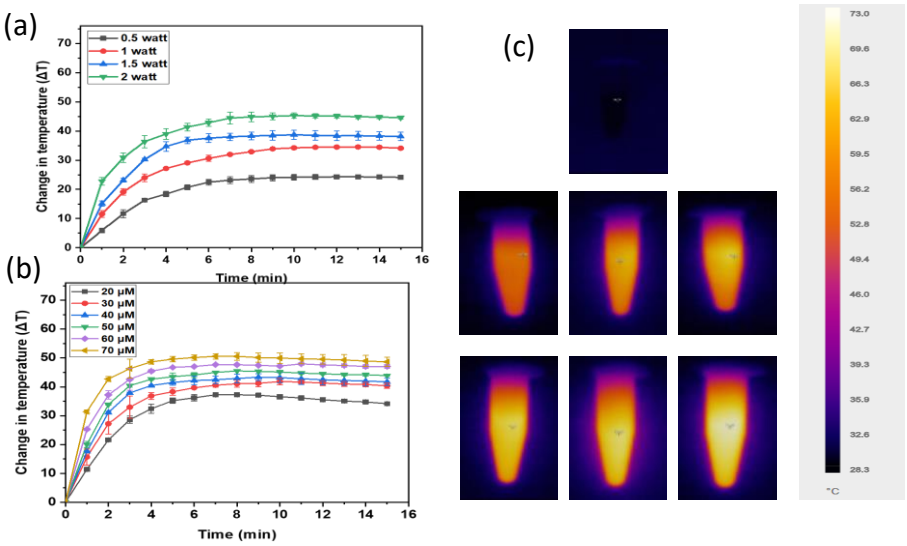

Figure 13. *ex vitro* photothermal temperature rise of (a) different concentrations of ICG J aggregates under constant dual-laser irradiation (808 nm + 915 nm) at a combined power of 1 watt. (b) ICG J aggregates (20 µM) under simultaneous dual-laser irradiation (808 nm + 915 nm) at different combined laser powers ranging from 0.5 to 2 watts. (c) IR thermal images of different concentrations of ICG J aggregates post dual-laser irradiation for 5 min each at constant

5.2.7 Cellular uptake

Fluorescence imaging revealed (Figure 14) that MDA-MB-231 breast cancer cells showed NIR emission of ICG J-aggregates, indicated by bright NIR fluorescence inside the cells after 6 hours of incubation.

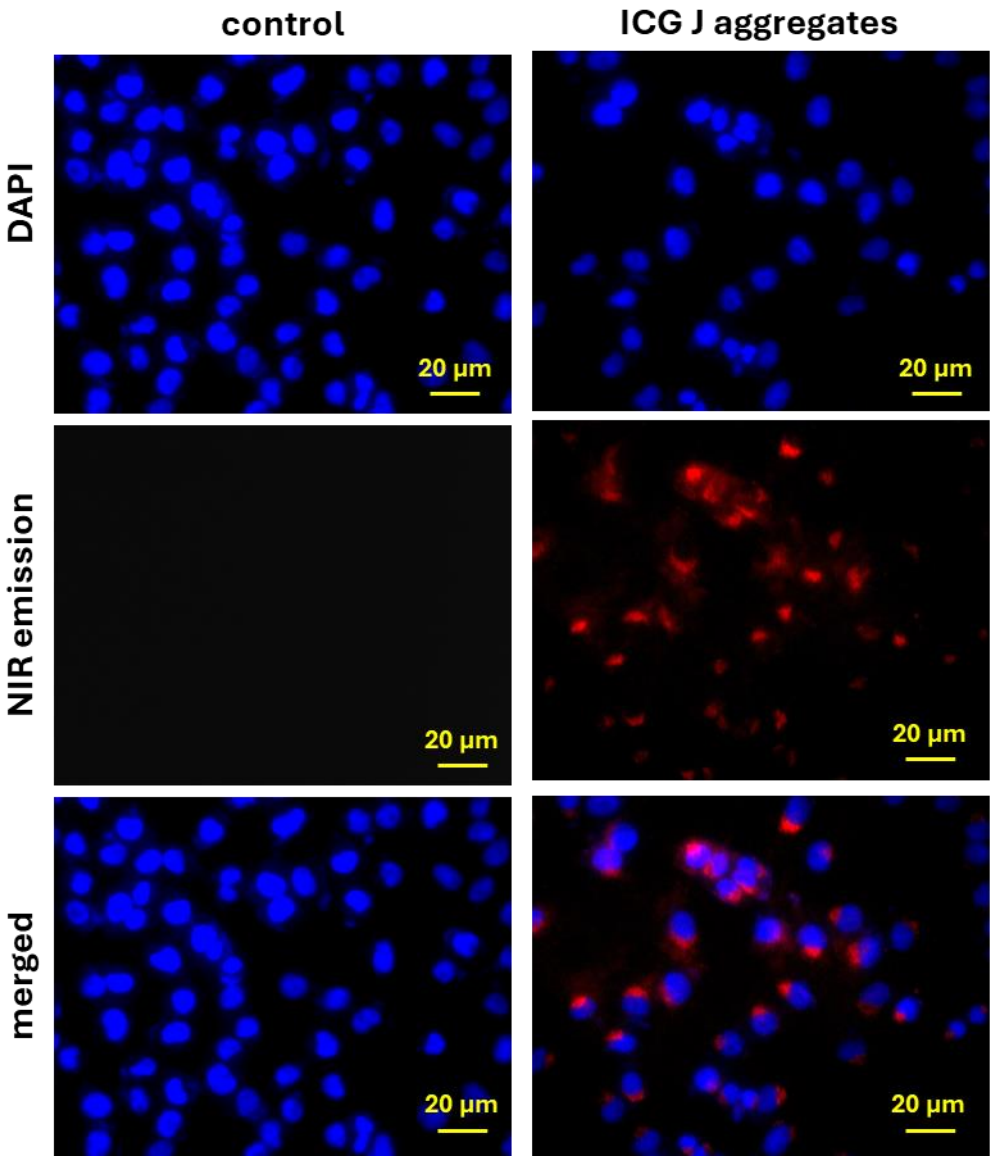

Figure 14. Cellular uptake of ICG J aggregates by MDA-MB-231 cells post 8 h of incubation.

5.2.8 In-Vitro Photothermal Therapy (PTT)

Figure 15 shows that when the J-aggregate-treated cells were exposed to dual-laser (808 nm + 915 nm) irradiation, a substantial photothermal effect was observed, leading to pronounced cancer cell killing. In comparison, cells treated with free ICG under identical laser conditions showed much lower levels of cell death, confirming that J-aggregates provide superior photothermal conversion and heat generation. This result highlights the efficient translation of the J-aggregates light absorption properties into localized thermal damage at the cellular level, demonstrating their strong therapeutic potential in vitro

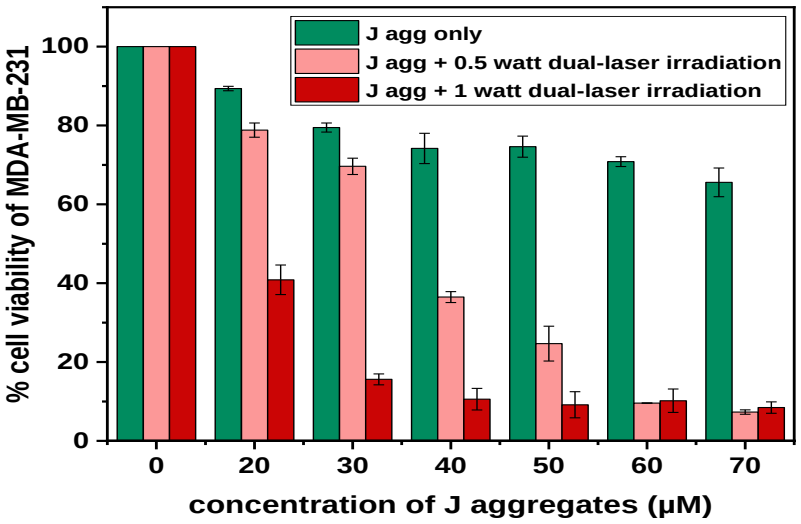

.

Figure 15 Percentage (%) cell viability of MDA-MB-231 cells treated with different concentrations of ICG J-aggregates, followed by (a) no laser (green bars) and (b) dual-laser irradiation (0.5 watt -pink bars and 1 watt red bars). Control cells, which were not treated with J aggregates, were also irradiated for 5 min to assess the effect of laser irradiation alone on the cells.

5.2.8. Live-Dead Assay

Live-dead staining (Figure 16) assays showed that untreated control cells and cells exposed only to laser irradiation remained largely viable,

with most cells staining green (live) (figure 16 (a) and (b)). In contrast, cells treated with J-aggregates and subjected to laser exposure showed a dramatic increase in PI-stained dead cells (red) (figure 16 (c) and (d)), confirming that the photothermal effect of the aggregates induced significant cytotoxicity. This clear difference between treated and control groups provides strong evidence that J-aggregates deliver efficient cancer cell ablation upon NIR laser activation.

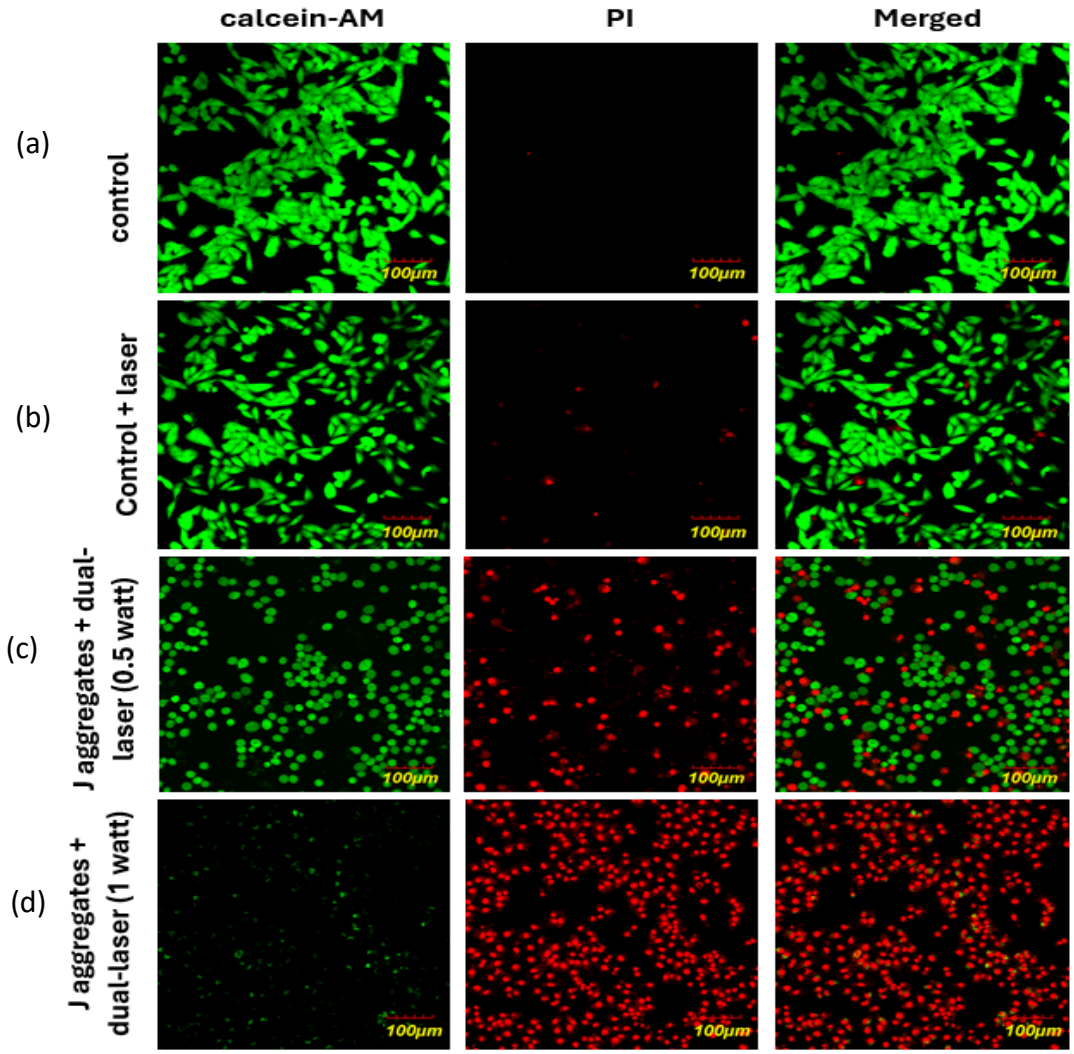

Figure 16. Live-dead assay of MDA-MB-231 cells done using calcein-PI co-staining. Cells were treated with (a) only media, (b) media + dual laser (808 nm + 915 nm), and J aggregates (20 µM) + dual laser (808 nm + 915 nm) at combined power of (c) 0.5-watt (d) 1 watt

Chapter-6

Conclusion and future scope

6.1 Conclusion

In this study, we successfully optimized, synthesized, and characterized indocyanine green (ICG) J-aggregates as potent photothermal agents for cancer therapy applications. Through a series of detailed experiments, we systematically characterized the physical, photophysical, and biological properties of these aggregates and compared their performance with free ICG, the FDA-approved monomeric dye traditionally used in medical imaging and experimental photothermal therapy (PTT). The findings from this work highlight the promising potential of ICG J-aggregates in overcoming several critical limitations associated with free ICG, such as poor photostability, poor aqueous solubility and rapid degradation, and limited photothermal efficiency.

Our results first established the optimal conditions for J-aggregate synthesis. Importantly, we observed that both insufficient (low) and excessive (high) temperatures disrupted the aggregation process, either due to kinetic limitations or thermal disassembly, respectively. Similarly, the incubation time was critical, with 24 hours being sufficient to reach aggregation equilibrium, while shorter or longer times led to suboptimal yields.

We also explored the stability of the synthesized J-aggregates under various conditions. The aggregates exhibited excellent storage stability when maintained at 4°C, retaining their optical and structural properties over several days, unlike free ICG, which degraded rapidly. We found that J-aggregates were also stable across physiological pH conditions, especially under mildly acidic environments similar to those found in the tumor microenvironment, which even promoted aggregation by reducing electrostatic repulsion between molecules. However, we noted that the aggregates were highly sensitive to organic solvents, such as ethanol, acetone, or DMSO, which caused rapid disassembly back to

monomeric ICG. This highlights the importance of maintaining aqueous environments for preserving aggregate integrity, which must be considered in future formulation strategies.

Importantly, we demonstrated that J-aggregates possess significantly enhanced photostability compared to free ICG. Under repeated or prolonged laser irradiation, J-aggregates maintained their absorbance intensity and thermal conversion efficiency, while free ICG photobleached and degraded. This photostability makes J-aggregates far more suitable for practical photothermal therapy, where multiple or extended laser exposure sessions are often required to achieve effective therapeutic outcomes.

Photothermal performance testing revealed that J-aggregates delivered superior light-to-heat conversion under both single-laser (915 nm) and dual-laser (808 + 915 nm) excitation, consistently outperforming free ICG. Notably, when we varied the power ratio between the two lasers while keeping the total power constant, the 1:1 ratio produced the highest temperature elevation, suggesting that balanced dual-wavelength excitation maximizes aggregate absorption and thermal output by efficiently engaging the full NIR absorbance profile. We also confirmed that both the concentration of J-aggregates and the applied laser power positively influenced thermal generation, with higher concentrations and higher power producing more robust heating. However, a saturation point was observed at very high dye concentrations, where additional loading no longer resulted in proportional thermal gain, likely due to light attenuation or self-shielding effects.

The biological studies provided further compelling evidence for the therapeutic potential of J-aggregates. Fluorescence microscopy confirmed that MDA-MB-231 breast cancer cells effectively internalized or bound J-aggregates, ensuring that sufficient photothermal agents were present at the cellular level. Importantly, the J-aggregates exhibited minimal dark toxicity, maintaining high cell

viability in the absence of laser exposure. When subjected to laser irradiation, however, J-aggregate-treated cells experienced substantial thermal damage and death, significantly exceeding the effects observed with free ICG or control treatments. Live-dead assays clearly visualized this impact, showing a pronounced shift from live (green) to dead (red) cells only in the J-aggregate + laser groups. SEM imaging further confirmed morphological evidence of photothermal damage, such as membrane rupture and blebbing, reinforcing the conclusion that J-aggregates deliver efficient, targeted cellular ablation upon NIR light activation.

Overall, this research provides a strong foundation for advancing ICG J-aggregates as next-generation photothermal agents for cancer therapy. The combination of optimized synthesis, robust stability, superior photothermal performance, and demonstrable in vitro therapeutic efficacy positions these nanostructures as highly promising candidates for further development.

6.2 Future scope

This research on indocyanine green (ICG) J-aggregates for photothermal therapy has the potential to revolutionize treatment of solid tumors. Cancer is one of the leading causes of death worldwide, and many current treatments like chemotherapy and radiation can be harsh, cause serious side effects, and may not always work. Photothermal therapy (PTT), which uses special light-absorbing agents to turn laser light into heat and kill cancer cells, offers a more targeted and less damaging approach. ICG J-aggregates, as studied in this project, show much better performance than regular ICG dye. They are more stable, absorb light more efficiently, and generate more heat when exposed to laser light. This means they could destroy tumors more precisely, with less harm to healthy tissues. In the future, using such materials could reduce patient pain, shorten recovery times, and improve treatment success rates[30].

ICG is already approved by FDA for medical imaging, so improving it through J-aggregates might make it better for treatments to patients.

Because photothermal therapy does not require large, expensive equipment like radiation machines, it has the potential to be used in hospitals and clinics even in low-income or rural areas. This could help reduce health inequalities by bringing advanced cancer treatments to people who otherwise would not have access.

In the bigger picture, this research supports the global fight against cancer to improve human health and well-being. It can reduce suffering, offer cancer patients more hope, and inspire future research and innovation. With continued effort, photothermal therapies like ICG J-aggregates may become a powerful tool to help save lives and improve the quality of life for patients around the world.

REFERENCES

1. Sung, H., et al., Global cancer statistics 2020: GLOBOCAN estimates of incidence and mortality worldwide for 36 cancers in 185 countries. CA: a cancer journal for clinicians, 2021. **71**(3): p. 209-249.
2. Rydén, L., et al., Epidermal growth factor receptor and vascular endothelial growth factor receptor 2 are specific biomarkers in triple-negative breast cancer. Results from a controlled randomized trial with long-term follow-up. Breast cancer research and treatment, 2010. **120**: p. 491-498.
3. A. Baudino, T., Targeted cancer therapy: the next generation of cancer treatment. Current drug discovery technologies, 2015. **12**(1): p. 3-20.
4. Tekade, M., et al., Recent advances in polymer-based nanomaterials for non-invasive photothermal therapy of arthritis. Pharmaceutics, 2023. **15**(3): p. 735.
5. Huang, X. and M.A. El-Sayed, Plasmonic photo-thermal therapy (PPTT). Alexandria journal of medicine, 2011. **47**(1).
6. Grosges, T. and D. Barchiesi, Gold nanoparticles as a photothermal agent in cancer therapy: the thermal ablation characteristic length. Molecules, 2018. **23**(6): p. 1316.
7. O'Neal, D.P., et al., Photo-thermal tumor ablation in mice using near infrared-absorbing nanoparticles. Cancer letters, 2004. **209**(2): p. 171-176.
8. Pérez-Hernández, M., et al., Dissecting the molecular mechanism of apoptosis during photothermal therapy using gold nanoprisms. ACS nano, 2015. **9**(1): p. 52-61.
9. Xiong, X., et al., A NIR light triggered disintegratable nanoplatform for enhanced penetration and chemotherapy in deep tumor tissues. Biomaterials, 2020. **245**: p. 119840.

10. Xu, C. and K. Pu, Second near-infrared photothermal materials for combinational nanotheranostics. Chemical Society Reviews, 2021. **50**(2): p. 1111-1137.
11. Salehpour, F., et al., Penetration profiles of visible and near-infrared lasers and light-emitting diode light through the head tissues in animal and human species: a review of literature. Photobiomodulation, photomedicine, and laser surgery, 2019. **37**(10): p. 581-595.
12. Zhu, S., et al., Near-infrared-II (NIR-II) bioimaging via off-peak NIR-I fluorescence emission. Theranostics, 2018. **8**(15): p. 4141.
13. Rodrigues, E.B., et al., Mechanisms of intravitreal toxicity of indocyanine green dye: implications for chromovitrectomy. Retina, 2007. **27**(7): p. 958-970.
14. Zeh, R., et al., The second window ICG technique demonstrates a broad plateau period for near infrared fluorescence tumor contrast in glioblastoma. PLoS One, 2017. **12**(7): p. e0182034.
15. Bhavane, R., et al., NIR-II fluorescence imaging using indocyanine green nanoparticles. Scientific reports, 2018. **8**(1): p. 14455.
16. Zhou, J.F., M.P. Chin, and S.A. Schafer. Aggregation and degradation of indocyanine green. in Laser Surgery: Advanced Characterization, Therapeutics, and Systems IV. 1994. SPIE.
17. Vincy, A., N. Bhatia, and R. Vankayala, Optical Characteristics of Indocyanine Green J-Aggregates Induced by Cisplatin for Phototheranostic Applications. ACS Biomaterials Science & Engineering, 2022. **8**(12): p. 5119-5128.
18. Chon, B., et al., Indocyanine green (ICG) fluorescence is dependent on monomer with planar and twisted structures and inhibited by H-aggregation. International Journal of Molecular Sciences, 2023. **24**(17): p. 13030.
19. Wood, C.A., et al., Clinically translatable quantitative molecular photoacoustic imaging with liposome-encapsulated ICG J-aggregates. Nature communications, 2021. **12**(1): p. 5410.

20. Rotermund, F., R. Weigand, and A. Penzkofer, J-aggregation and disaggregation of indocyanine green in water. Chemical physics, 1997. **220**(3): p. 385-392.
21. Bricks, J.L., et al., Fluorescent J-aggregates of cyanine dyes: basic research and applications review. Methods and applications in fluorescence, 2017. **6**(1): p. 012001.
22. Changalvaie, B., et al., Indocyanine green J aggregates in polymersomes for near-infrared photoacoustic imaging. ACS applied materials & interfaces, 2019. **11**(50): p. 46437-46450.
23. Xu, S., et al., Recent progress in utilizing near-infrared J-aggregates for imaging and cancer therapy. Materials Chemistry Frontiers, 2021. **5**(3): p. 1076-1089.
24. Ohno, O., Y. Kaizu, and H. Kobayashi, J-aggregate formation of a water-soluble porphyrin in acidic aqueous media. The Journal of chemical physics, 1993. **99**(5): p. 4128-4139.
25. Chen, C., et al., Metal ions-bridged J-aggregation mediated nanoassembly composition for breast cancer phototherapy. Asian Journal of Pharmaceutical Sciences, 2022. **17**(2): p. 230-240.
26. Branca, C. and G. D'Angelo, Aggregation behavior of pluronic F127 solutions in presence of chitosan/clay nanocomposites examined by dynamic light scattering. Journal of Colloid and Interface Science, 2019. **542**: p. 289-295.
27. Fylymonova, I., S. Yefimova, and A. Sorokin, The formation of J-aggregates in solutions of reverse micelles. Functional materials, 2012.
28. Song, X., et al., Nano-assemblies of J-aggregates based on a NIR dye as a multifunctional drug carrier for combination cancer therapy. Biomaterials, 2015. **57**: p. 84-92.
29. Kumari, P., et al., Tailoring indocyanine green J-aggregates for imaging, cancer phototherapy, and drug delivery: a review. ACS Applied Bio Materials, 2024. **7**(8): p. 5121-5135.

30. Alotaibi, H. and T. Hatahet, Indocyanine green J-aggregate (IJA) theranostics: Challenges and opportunities. International Journal of Pharmaceutics, 2024: p. 124456.